# Thermodynamic Optimization of Water-Cooled Infrastructure for Vehicle Lithium–Ion Battery Based on Exergy

Hetong Xu,* Liang Guo,† and Hao Tian‡
*Chinese Academy of Sciences, 130033 Changchun, Jilin, People's Republic of China*
and
Chuiyu Pan§
*China FAW Group Corporation New Energy Vehicle Branch, 130122 Changchun, Jilin, People's Republic of China*

https://doi.org/10.2514/1.T5824

**Electric vehicle technology is developing rapidly with the attention of energy and environmental issues, lithium–ion batteries as the important component are widely used for their superior performance. However, batteries generate a lot of heat during operation. If not cooled in time, heat will accumulate in the battery package, causing a rapid temperature rise and an increasing temperature nonuniformity. Thermodynamic analysis based on the least exergy dissipation principle is to optimize both the configuration and operating strategy of a water-cooled system for the vehicle lithium–ion battery packages. Four typical structures and 24 packages of 96 lithium–ion single batteries from an e-powered SUV were designed and tested to verify the exergy-based optimization. The test results showed a good agreement with the theoretical analysis and prediction. Under various battery discharging conditions, the best thermal performance was observed when the cooling water was inlet to the middle-positioned battery packages, at which the measured maximum temperature gradient among the 24 battery packages can be controlled within 3.1 K, much lower than the other three configurations, and the measured peak temperature was 1.1–5.9 K lower than the other three configurations.**



## Nomenclature

| | | |
|---|---|---|
| $A$ | = | effective area for heat dissipation of each battery package |
| $c_p$ | = | specific heat of water |
| $D$ | = | equivalent hydraulic diameter of water channel inside the cooling panel |
| $f$ | = | frictional coefficient of water flow inside the cooling panel |
| $h$ | = | convective heat transfer coefficient |
| $L$ | = | length of the cooling panel |
| $m$ | = | water mass flow rate |
| $Q$ | = | heat dissipated by each battery package |
| $S_t$ | = | Stanton number |
| $T$ | = | mean temperature of the lithium-ion battery package |
| $\overline{T}_a$ | = | mean water temperature along the cooling panel |
| $T_a$ | = | temperature of the inlet cooling water |
| $T_o$ | = | temperature of the outlet water |
| $V$ | = | mean water velocity across the cooling panel |
| $\rho$ | = | water density |
| $\Psi_{\text{flow}}$ | = | exergy loss of flow resistance |
| $\Psi_{\text{heat}}$ | = | exergy loss of thermal resistance |
| $\Psi_{\text{total}}$ | = | total exergy loss |

Received 14 June 2019; revision received 9 September 2019; accepted for publication 16 October 2019; published online 29 November 2019. 

*Master's Candidate, Thermal Control Group, Changchun Institute of Optics, Fine Mechanics and Physics; also University of Chinese Academy of Sciences, Beijing, China; Pro_xuht@126.com.

†Associate Professor, Thermal Control Group, Changchun Institute of Optics, Fine Mechanics and Physics; guoliang@ciomp.ac.cn.

‡Associate Professor, Thermal Control Group, Changchun Institute of Optics, Fine Mechanics and Physics; tianh@ciomp.ac.cn (Corresponding Author).

§Associate Professor, R&D; panchuiyu@faw.com.cn.

## I. Introduction

THE structures of several typical lithium-ion batteries and packaging configurations are illustrated in Figs. 1a–1d [1,2]. The pack level (Fig. 1d) is the most widely used battery packaging in lithium-powered vehicles. Most cooling designs are based on this pack model (e.g., dozens of sensors and cooling ducts integrated into the battery pack network).

Lithium-ion batteries generate a lot of heat during charging and discharging; different thermal environments also affect the performance of lithium-ion batteries [3–5]. Therefore, it is important to dissipate heat from batteries. For the state of the art, air cooling, liquid cooling, and phase-change cooling take predominating current battery thermal management (BTM) research [6,7]. Many research efforts have been made on the optimization of cooling configuration (e.g., flow model, fluid parameters, cooling channel layout, and integrated design [8–39]) to enhance heat transfer and to improve temperature uniformity among the integrated battery packages (e.g., airflow path comparison, as demonstrated in Fig. 2) [8]. Others attempted to combine a special phase-change material (PCM) into a battery pack network to get a better thermal shock response, a lower peak temperature, and less cooling cost, at various battery charging/discharging rates and package currents [40–54]. Another important work is to develop an appropriate theoretical model (e.g., heat generation model, electrochemical model, and equivalent circuit model [55–72]) to perform a more precise quantitative analysis on battery chemical-thermal characteristics and to better assist BTM design.

Thermodynamic method (e.g., exergy model) is another appropriate approach to perform a quantitative analysis and an effective optimization on heat transfer and thermal flow network [73–77]. The overwhelming advantage of using an exergy analysis (e.g., the unique ability to get an analytical solution of optimum flow parameter and optimal operating strategy, other than the large-scale simulation by computational fluid dynamics or finite element method software, quite time efficient) fits the BTM research.

To obtain better temperature distribution, uniformity, and lower cooling energy consumption, the theory of exergy loss based on the second law of thermodynamics is used to quantitatively calculate and evaluate the quality loss of energy during lithium-ion battery charging and discharging, and quantitative analysis and comparison of thermodynamic properties. In addition, we also obtain the optimal lithium-ion BTM strategy through optimization.

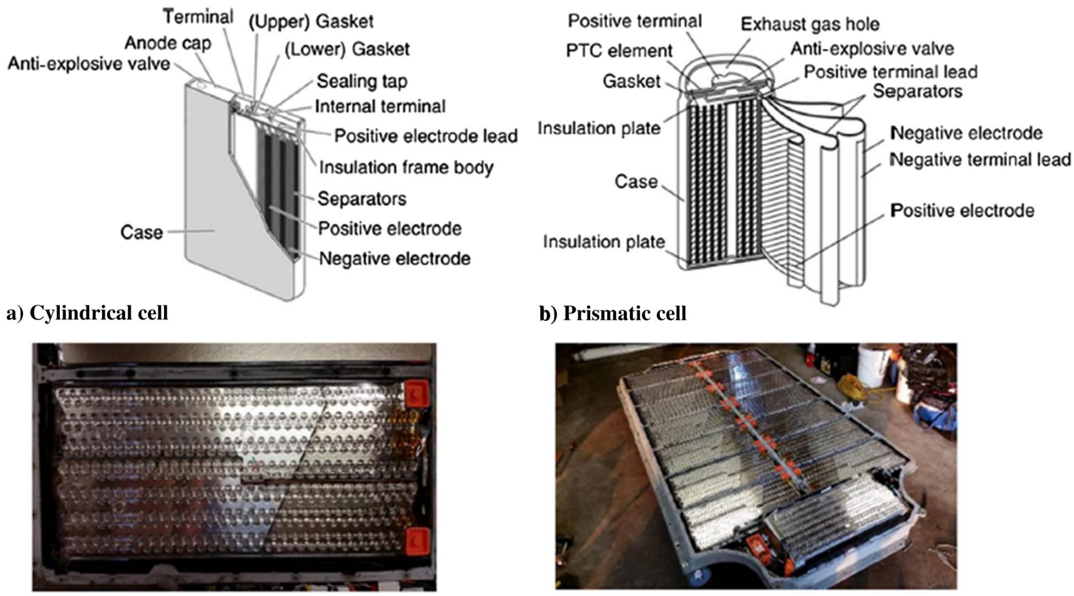


**a) Cylindrical cell** **b) Prismatic cell**

**c) Module level** **d) Pack level**

**Fig. 1 Schematics and pictures of different battery configurations: a) cylindrical cell, b) prismatic cell, c) module level, and d) pack level [1,2] (PTC, positive temperature coefficient).**

## II. Exergy Analysis Model

Shah [73] analyzed the exergy loss during water flow and heat transfer, and found that, as water flows across the motherboard, exergy is consumed by both thermal and flow resistance between water and the motherboard surface. The total exergy loss can be calculated as follows [72]:

$$\Psi_{\text{total}} = \Psi_{\text{heat}} + \Psi_{\text{flow}} = \frac{Q^2}{Lmc_p}\frac{D}{S_t}\frac{T_a}{\overline{T_a}^2} + \frac{8m^3L}{\rho^2}\frac{f}{DA^2}\frac{T_a}{\overline{T}_a} \tag{1}$$

$Q$ is the heat dissipated by each battery package (in W); $T_a$ is the temperature of the inlet cooling water (in K); $\overline{T}_a$ is the mean water temperature along the cooling panel, which is commonly calculated using Eq. (2) (in K); $m$ is the water mass flow rate (in kg/s); $c_p$ is the specific heat of water [in $J/(kg \cdot K)$]; $\rho$ is the water density ($kg/m^3$); $L$ is the length of the cooling panel (in m); $D$ is the equivalent hydraulic diameter of the water channel inside the cooling panel (in m); $A$ is the effective area for heat dissipation of each battery package (in $m^2$); $f$ is the mean frictional coefficient of water flow inside the cooling panel; and $St$ is the Stanton number, as calculated by Eq. (3):

$$\overline{T_a} = T_a + \frac{(T - T_a) - (T - T_o)}{\ln(T - T_a/T - T_o)} \tag{2}$$

$T$ is the mean temperature of the lithium-ion battery packages (in K); $T_o$ is the temperature of the outlet water (in K):

$$S_t = \frac{h}{\rho V c_p} \tag{3}$$

in which $h$ is the convective heat transfer coefficient [in $W/(m^2 \cdot K)$]; $V$ is the mean water velocity across the cooling panel (in m/s); and $Q$, $h$, and $T - \overline{T}_a$ are governed by Newton's law of cooling, expressed by Eq. (4):

$$Q = hA(T - \overline{T}_a) \tag{4}$$

Bring Eqs. (3) and (4) and $m = (\pi/4)(\rho V D^2)$ into Eq. (1) to get

$$\Psi_{\text{total}} = \Psi_{\text{heat}} + \Psi_{\text{flow}} = \frac{4A}{\pi DL}\frac{(T - \overline{T}_a)T_a}{\overline{T}_a^2}Q + \frac{8m^3L}{\rho^2}\frac{f}{DA^2}\frac{T_a}{\overline{T}_a} \tag{5}$$

Equation (5) is the final expression for the calculation of total exergy loss $\Psi_{\text{total}}$ during heat transfer between each battery package and the corresponding cooling panel [7]. When the dissipated heat $Q$ and panel length $L$ can be assumed constant, the total exergy loss of the battery cooling process can be calculated using Eq. (5). Figure 3 shows a comparison of the normalized exergy dissipation ($\Delta E_x/\Delta E_{x,\max}$) with the normalized temperature($T_{\text{battery}}/T_{\text{battery,max}}$) of the battery package for a single cooling panel (package heat $Q = 30$ W; panel area $A = 0.12$ $m^2$) with inlet water temperatures $T_{\text{in}}$ of 278, 283, 293, and 300 K, and water velocity of 0.1–1.0 m/s.

It can be seen from Fig. 3 that, for a given heat $Q$ and panel area $A$, the optimal water velocity (or optimum flow rate), which corresponds to the minimum exergy loss, changes with water inlet temperature (also designated as the reference temperature for zero-exergy state). In other words, the point with minimum exergy loss, which is the lowest point in the exergy dissipation curve in Fig. 3, corresponds to the optimal thermodynamic performance based on the exergy analysis. In addition, for a given water velocity, both values of normalized

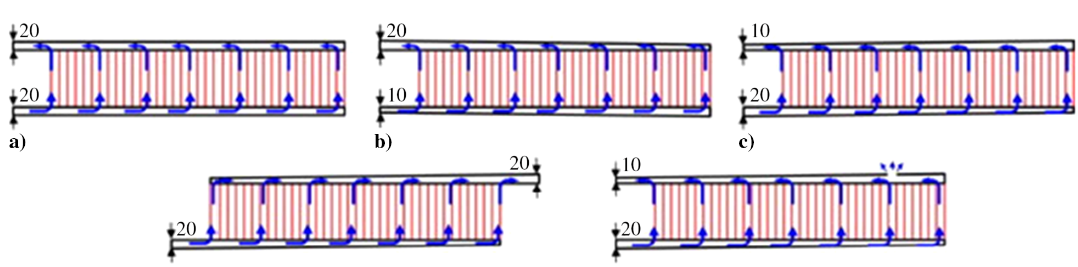


**Fig. 2 Comparison of different designs of inlet and outlet ducts [8].**

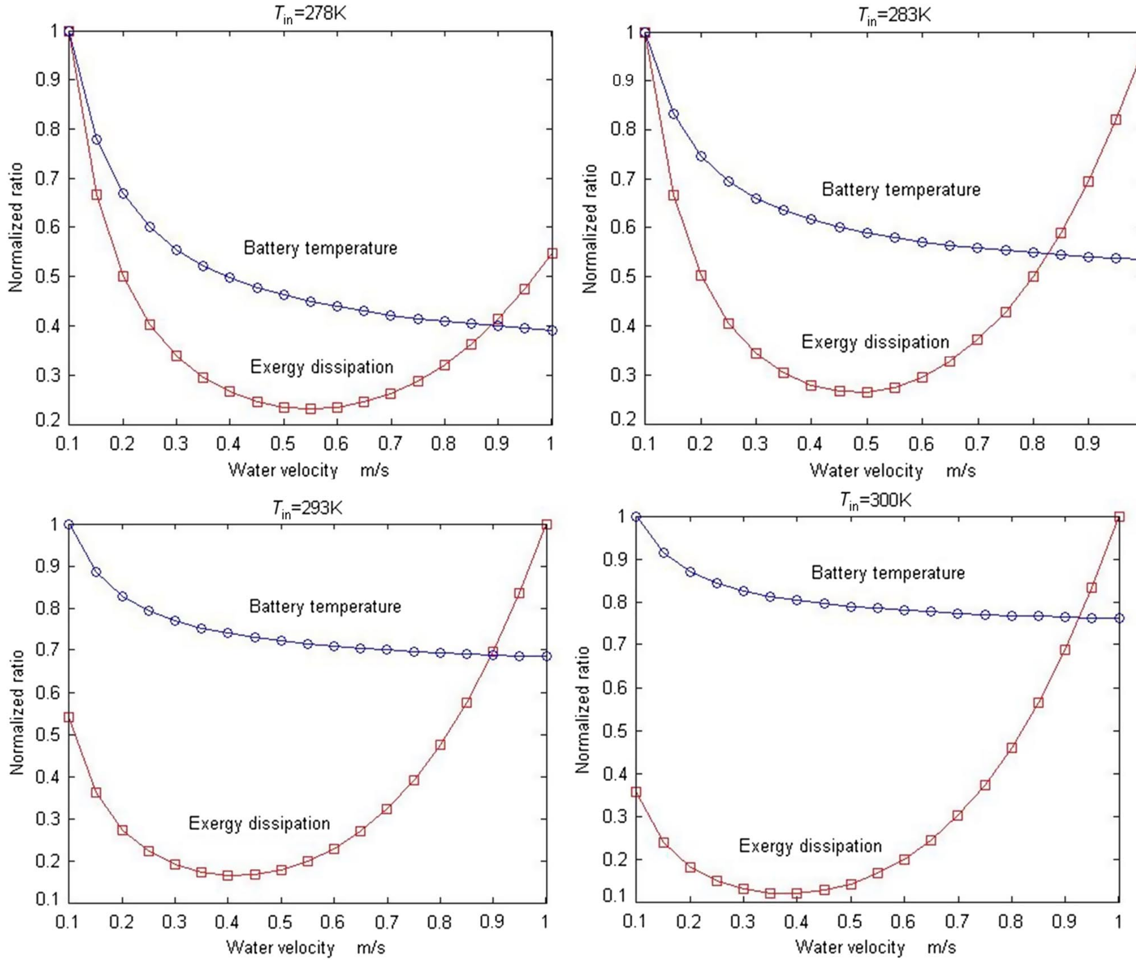


**Fig. 3 Normalized exergy performance compared with cooling performance.**

exergy loss and battery surface temperature vary with inlet water temperature (zero-exergy state temperature). This indicates a strong possibility to get an optimal cooling design for each given condition, through the optimization based on the least exergy dissipation analysis.

Figure 4 shows the calculation of the performance of the battery package and the pump, with the optimum velocity range (0.35–0.55 m/s) suggested by the least exergy dissipation analysis, which is shown in the figure as the red region. For each optimum water velocity, the corresponding battery temperature ranges from 280 to 305 K, which is only 0.8–2.5 K higher than the lowest temperature in each cooling condition ($T_{in}$). This indicates a quite acceptable thermal performance of the battery package.

Similarly, for each exergy optimum velocity, the pump efficiency correspondingly ranges from 0.72 to 0.88 (maximum of 0.92), with the normalized power that ranges from 0.45 to 0.63 (maximum of 0.90); both indicate a satisfactory power performance of the pump.

The preceding analysis on a single-panel-package case proves the least exergy dissipation principle for optimization and optimal design of battery cooling infrastructure. For a large-scale network containing multicooling panels and battery packages, it has been proved that [11], with the same boundary conditions, both the optimal thermal performance and optimum energy performance occur with the least exergy dissipation state of the whole network. Therefore, the basic

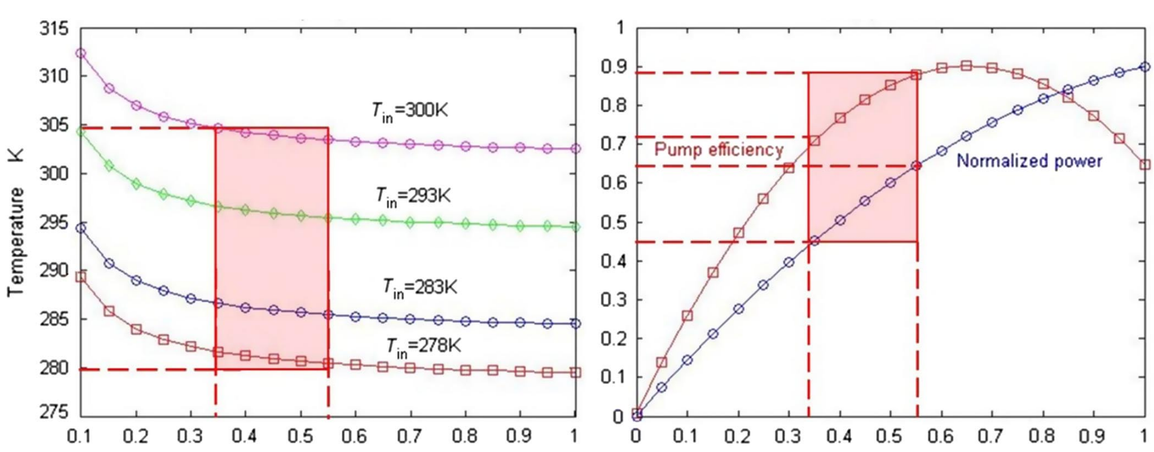


**Fig. 4 Performance of battery and pump at the optimum velocity suggested by the exergy analysis.**

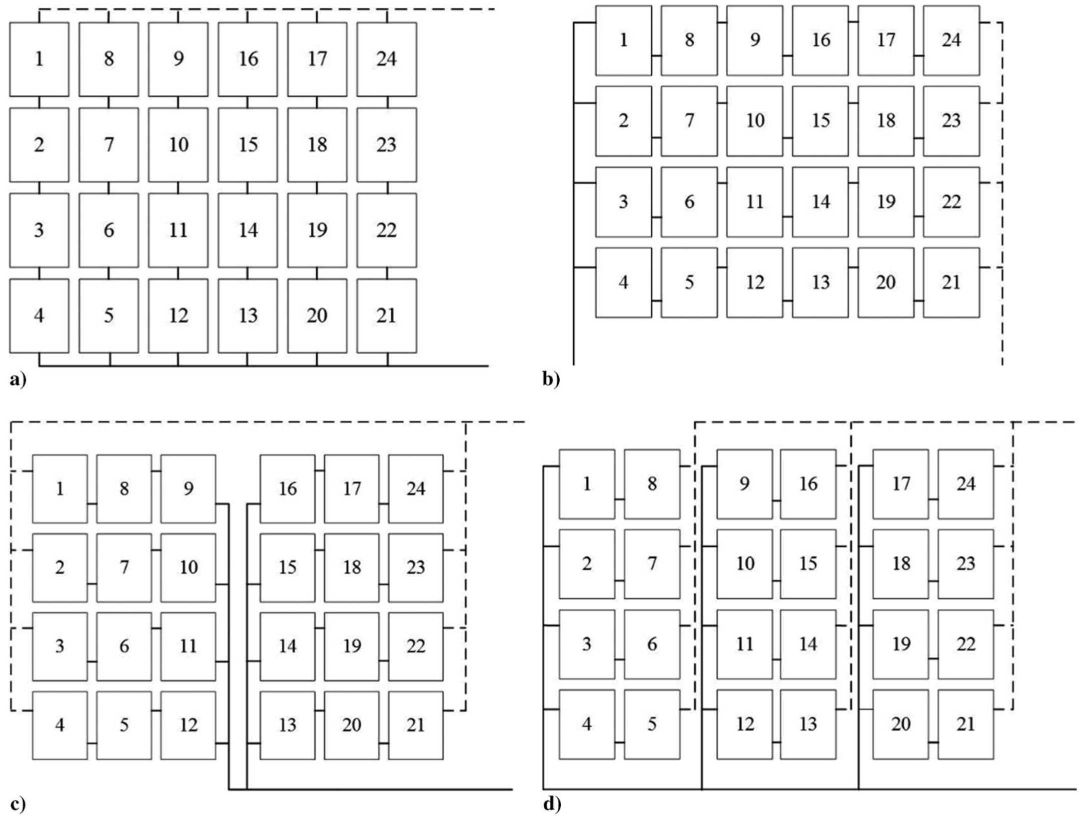


**Fig. 5 Four typical water-cooled configurations for the lithium battery package.**

theoretical tool for the optimal cooling design of multibattery packages is the exergy analysis model.

## III. Design of Water Cooling Infrastructure

Four typical structures of water-cooled panels were designed and are illustrated in Figs. 5a–5d , in which the bold solid line represents the main pipe for the water inlet, whereas the dashed line represents the main pipe for the water outlet. All 24 cooling panels were numbered in sequence.

For the state of the art, the cooling configurations (Figs. 5a and 5b) are commonly used in a vehicle BTM system. The third and fourth layouts (Figs. 5c and 5d) are designed to improve the temperature uniformity and cooling efficiency around the middle-positioned battery packages (numbered 10, 11, 14, and 15), which have been measured and observed as the most likely overheated regions [12].

**Table 1 Information of lithium-ion power battery packages**

| Items | Parameters |
|---|---|
| Type of lithium–ion power battery package | Lithium-ion cylindrical battery of 18650 |
| Product compliant | Restriction of Hazardous Substances |
| Model of battery packages | INR18650 7S16P (25.2 V; 51.2 A) |
| Battery cell | INR18650 (3200 mAh DLG) |
| Assemble style | 7S16P + PCM + socket |
| Assembly drawing | See Fig. 6 |

**Table 2 Testing conditions of water cooling**

| Items | Parameters |
|---|---|
| Number of battery packages and panels | 24 (6 × 4; see Fig. 7) |
| Inlet water temperature, K | 283, 293, and 300 |
| Battery discharge temperature, K | 273, 300, and 313 |
| Battery discharge ratio | 1*C* and 3*C* |
| Water velocity, m/s | 0.1–1.0 |
| Package configuration | See Fig. 5 |

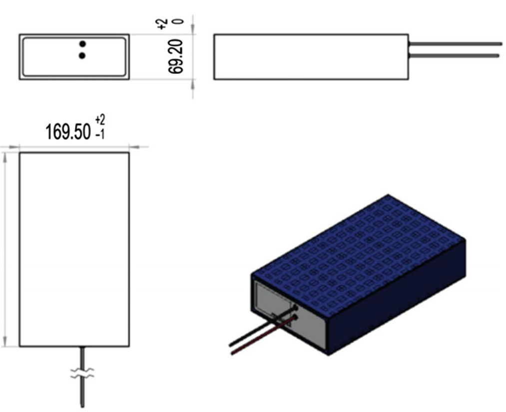


**Fig. 6 Assembly drawing of a package unit of 18650-type lithium-ion battery.**

## IV. Case Study

For each cooling configuration in Fig. 5, the corresponding optimal operating mode and the optimum performance were analyzed, tested, and compared using the least exergy dissipation model.

### A. Testing Condition

To perform a fair comparison, a uniform reference temperature of zero-exergy state was set to be the lowest temperature of the entire heat transfer network, which was the inlet temperature of cooling water. To demonstrate the least exergy dissipation model, three typical temperature conditions ($T_{in}$ = 283, 293, and 300 K) combined with several commonly used battery discharge conditions have been measured and compared.

The testing condition in detail is listed in Tables 1 and 2, and shown in Fig. 6.

a) Cold-water pipe

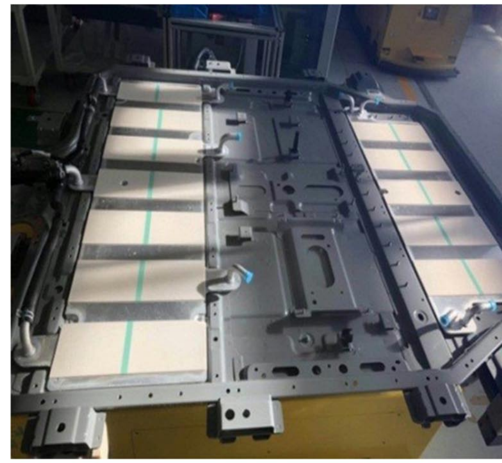

b) Cold-water plate

**Fig. 7 Assembled lithium-ion power battery packages and water-cooled panels.**

Figures 7 and 8 show the photographs of 24 battery packages and 24 cooling panels assembled in an integrated testing platform. The equipment named e-Storage System in Figs. 8a and 8b was used to test the current, voltage, and power of the battery under different operating conditions, such as different discharge rates and different ambient temperatures. The device from TOPRIE, shown in Figs. 8c and 8d , was used to measure and monitor the battery packages.

### B. Result Analysis

Figure 9 shows the fitted discharge curve of a single 18650-type lithium-ion battery under $1C$ (3 A for 3600 s at 300 K) and $3C$ (9 A for 1200 s at 300 K) conditions, based on measured voltage data in each testing condition.

Using the fitted curve, cases in Fig. 3 have been recalculated, with varied discharged heat (not a fixed value $Q$) and varied discharged rate ($1C$ and $3C$). The result of the normalized exergy dissipation is illustrated in Fig. 10.

Compared with the exergy loss curve in Fig. 3, Fig. 10 shows a similar trend of exergy dissipation, optimum velocity occurs at 0.3–0.5 m/s at which least exergy is dissipated. This proves the feasibility of using a least exergy dissipation model to analyze and optimize the actual discharge characteristics of lithium-ion battery packages.

Based on the optimum water velocity suggested by the least exergy dissipation model, under $1C$ and $3C$ discharge conditions, Figs. 11 and 12 give the theoretically optimal temperature distribution of the 24 battery packages for each configuration in Fig. 4 (solid lines), and compare them with the actual measured values (marked by circles and squares). During the test, two temperature sensors were placed both on the positive and negative electrodes of each single battery, and so there were 192 ($24 \times 4 \times 2$) sensors for measuring the temperature of the battery packages in the system. The circles and squares in the figure represent the maximum and minimum temperature values returned by 192 temperature sensors at the same moment. The inlet temperature of cooling water remained constant for each configuration.

a) E-storage device


b) E-storage device

c) Device from TOPRIE


d) Display screen

**Fig. 8 Photographs of integrated testing platform for the lithium-ion battery packages.**

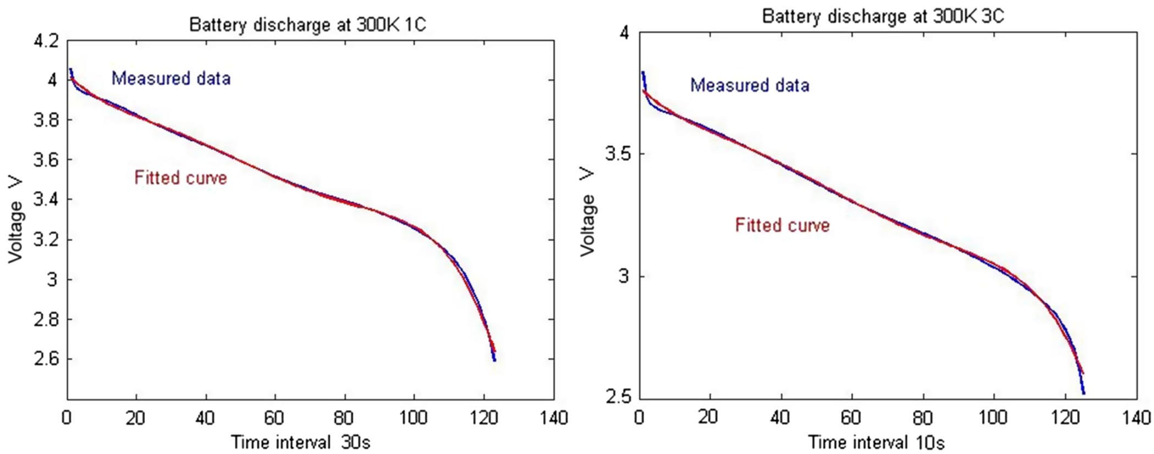


**Fig. 9 Fitted battery discharge curve based on measured voltage data.**



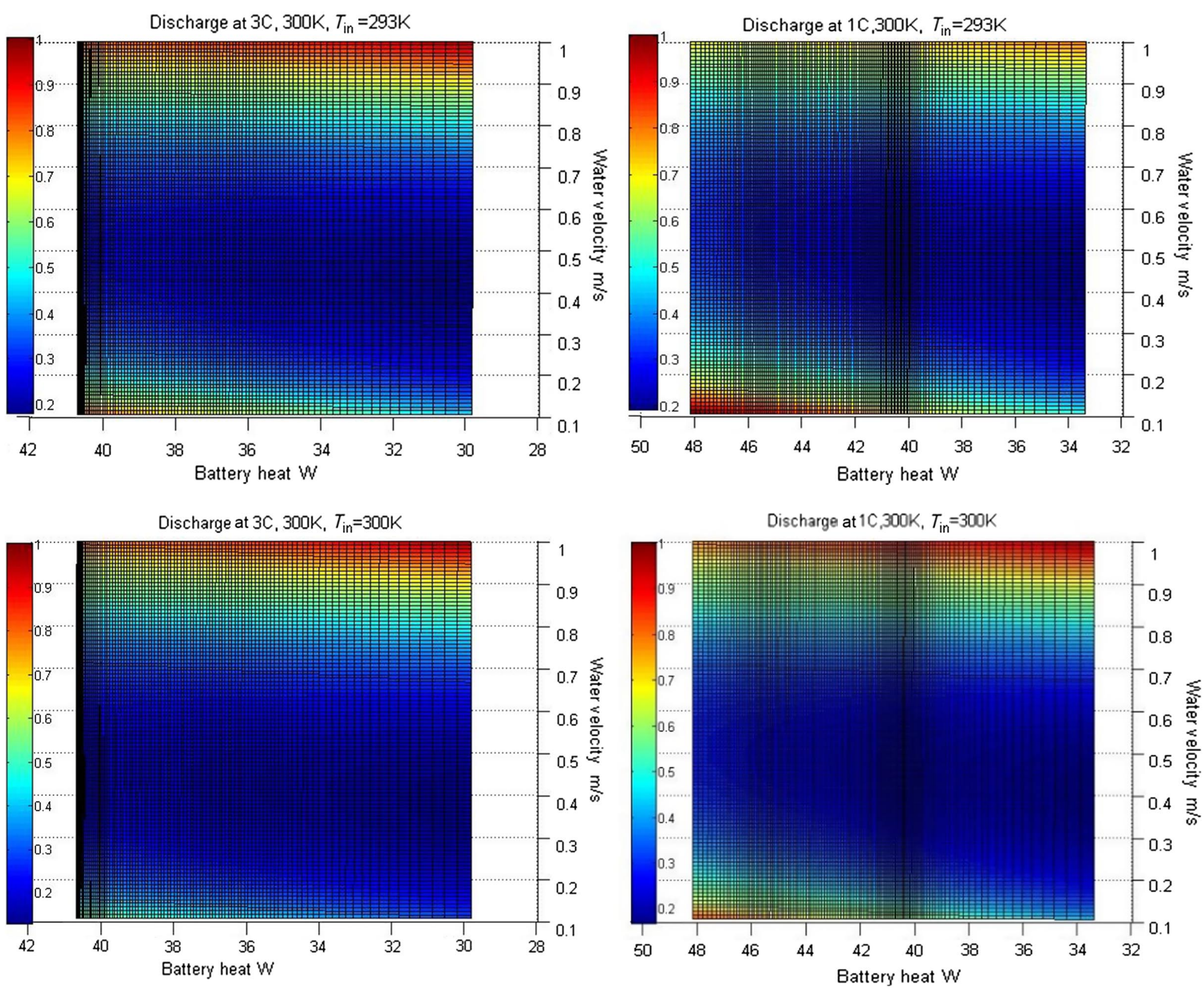


**Fig. 10 Normalized exergy dissipation at different battery discharge rates and water flow rates.**

Figures 11 ($3C$; $T_{in} = 285$ K) and 12 ($1C$; $T_{in} = 290$ K) show a good agreement of battery temperature between the optimized values given by the exergy analysis and the measured values for each configuration suggested in Fig. 5, with the maximum error, which is the maximum difference between the theoretically predicted value and the experimental value, of 0.3 K. The least exergy dissipation method for battery cooling optimization has been verified.

The thermodynamic parameters of the four structures were calculated and are listed in Tables 3 and 4.

It can be seen that, under the same discharging and cooling conditions, the third configuration, illustrated in Fig. 5c , shows the best thermal performance. For discharge at $1C$ rate, the maximum battery temperature of the third configuration (Fig. 5c) is 1.1 K lower than the other three configurations. The largest temperature gradient,

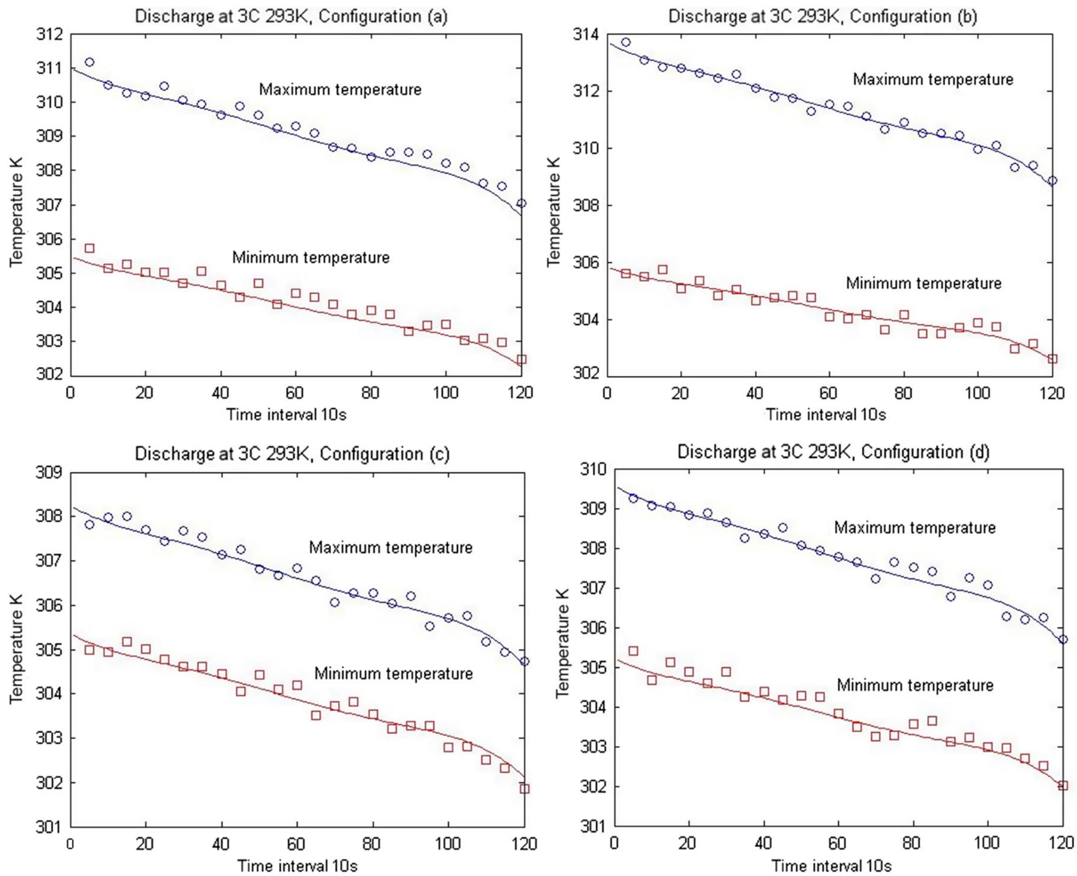


Fig. 11 Optimal battery temperature curve at corresponding optimum water velocity.

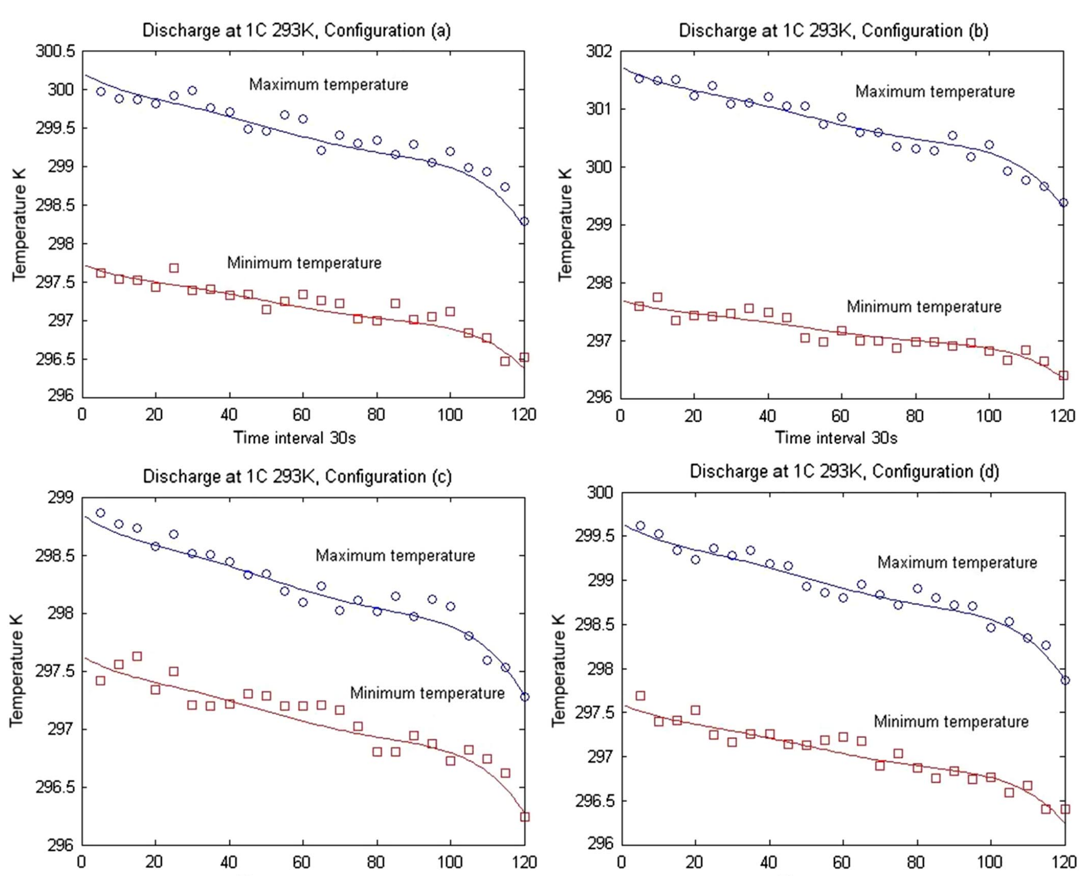


Fig. 12 Optimal battery temperature curve at corresponding optimum water velocity.

**Table 3 Thermodynamic parameters of four structures under 3*C* and 285 K**

| Structure | Maximum temperature, K | Maximum temperature gradient, K | Exergy loss, W |
|---|---|---|---|
| a | 311.2 | 5.5 | 50.53 |
| b | 313.7 | 8.1 | 52.76 |
| c | 307.8 | 3.1 | 47.22 |
| d | 309.3 | 4.4 | 48.43 |

**Table 4 Thermodynamic parameters of four structures under 1*C* and 290 K**

| Structure | Maximum temperature, K | Maximum temperature gradient, K | Exergy loss, W |
|---|---|---|---|
| a | 300 | 2.6 | 7.06 |
| b | 301.5 | 4.2 | 7.52 |
| c | 298.9 | 1.5 | 6.51 |
| d | 299.6 | 2.2 | 6.78 |

which is defined as the largest difference between the battery location with the maximum measured temperature and the location with the minimum measured temperature at the same moment, is 1.5 K, much smaller than the other three 8.1 K. The exergy loss, 47.22 W, is also the smallest. The situation is the same for discharge at 3*C* rate. The inlet water to the middle eight packages (numbered 9–16 in Fig. 5) not only led to the best temperature uniformity, but it also made the lowest peak temperature among the 24 packages. Such configuration is recommended for future lithium-ion battery cooling design.

## V. Conclusions

As stated previously, the water cooling process of lithium-ion battery packages can be analyzed and optimized using the exergy theory (e.g., the least exergy dissipation principle). Some major conclusions are summarized as follows:

1) For a given heat and panel area, the optimal water velocity (or flow rate) corresponds to both the minimum exergy loss and the high pump efficiency range during the heat transfer process from the battery package to the cooling water.

2) Thermal performance (e.g., exergy dissipation) changes with water inlet temperature and battery discharge condition (e.g., discharging rate and temperature).

3) The inlet water to the middle-positioned packages generates better temperature uniformity (e.g., largest temperature gradient less than 3.1 K and lower peak temperature (1.1–5.6 K lower than other cooling configurations).

4) The maximum error between the exergy calculated temperature and the measured values is smaller than $\pm 0.3$ K, under each testing condition.

## Acknowledgments

This work was supported by the National Natural Science Foundation of China (grant number 61605203) and the Youth Innovation Promotion Association of the Chinese Academy of Sciences (grant number 2015173). The authors would like to acknowledge Liang Guo for his help with this paper.

## References

[1] Blomgren, G. E., “The Development and Future of Lithium-Ion Batteries,” *Journal of the Electrochemical Society*, Vol. 164, No. 1, 2017, pp. A5019–A5025.
https://doi.org/10.1149/2.0251701jes

[2] Anon., “Pics/Info: Inside the Battery Pack,” *Tesla Motors Club* [online database], https://teslamotorsclub.com/tmc/threads/pics-info-inside-the-battery-pack.34934/ [retrieved 20 Aug. 2014].

[3] Gao, T., Wang, Z., Chen, S., and Guo, L., “Hazardous Characteristics of Charge and Discharge of Lithium-Ion Batteries Under Adiabatic Environment and Hot Environment,” *International Journal of Heat and Mass Transfer*, Vol. 141, Oct. 2019, pp. 419–431.
https://doi.org/10.1016/j.ijheatmasstransfer.2019.06.075

[4] Jiang, F., Liu, K., Wang, Z., Tong, X., and Guo, L., “Theoretical Analysis of Lithium-Ion Battery Failure Characteristics Under Different States of Charge,” *Fire and Materials*, Vol. 42, No. 6, 2018, pp. 680–686.
https://doi.org/10.1002/fam.v42.6

[5] Wang, Z., Tong, X., Liu, K., Shu, C.-M., Jiang, F., Luo, Q., and Wang, H., “Calculation Methods of Heat Produced by a Lithium-Ion Battery Under Charging-Discharging Condition,” Vol. 43, No. 2, 2019, pp. 219–226.
https://doi.org/10.1002/fam.2690

[6] Conte, F. V., “Battery and Battery Management for Hybrid Electric Vehicles: A Review,” *Elektrotechnik Und Informationstechnik*, Vol. 123, No. 10, 2006, pp. 424–431.
https://doi.org/10.1007/s00502-006-0383-6

[7] Pesaran, A., and Santhanagopalan, S., “Addressing the Impact of Temperature Extremes on Large Format Li-Ion Batteries for Vehicle Applications,” National Renewable Energy Lab. Rept. NREL/PR-5400-58145, Golden, CO, March 2013.

[8] Park, H., “A Design of Air Flow Configuration for Cooling Lithium Ion Battery in Hybrid Electric Vehicles,” *Journal of Power Sources*, Vol. 239, Oct. 2013, pp. 30–36.
https://doi.org/10.1016/j.jpowsour.2013.03.102

[9] Mohammadian, S. K., He, Y. L., and Zhang, Y., “Internal Cooling of a Lithium-Ion Battery Using Electrolyte as Coolant Through Microchannels Embedded Inside the Electrodes,” *Journal of Power Sources*, Vol. 293, Oct. 2015, pp. 458–466.
https://doi.org/10.1016/j.jpowsour.2015.05.055

[10] Chen, Y., and Evans, J. W., “Thermal Analysis of Lithium-Ion Batteries,” *Journal of Electrochemical Society*, Vol. 143, No. 9, 1996, pp. 2708–2712.
https://doi.org/10.1149/1.1837095

[11] Bandhauer, T. M., and Garimella, S., “Passive, Internal Thermal Management System for Batteries Using Microscale Liquid-Vapor Phase Change,” *Applied Thermal Engineering*, Vol. 61, No. 2, 2013, pp. 756–769.
https://doi.org/10.1016/j.applthermaleng.2013.08.004

[12] Giuliano, M. R., Advani, S. G., and Prasad, A. K., “Thermal Analysis and Management of Lithium-Titanate Batteries,” *Journal of Power Sources*, Vol. 196, No. 15, 2011, pp. 6517–6524.
https://doi.org/10.1016/j.jpowsour.2011.03.099

[13] Kelly, K. J., Mihalic, M., and Zolot, M., “Battery Usage and Thermal Performance of the Toyota Prius and Honda Insight During Chassis Dynamometer Testing,” *17th Annual Battery Conference on Applications and Advances*, Vol. 1, IEEE, New York, 2006, pp. 247–252.
https://doi.org/10.1109/BCAA.2002.986408

[14] Liu, H., Wei, Z., He, W., and Zhao, J., “Thermal Issues About Li-Ion Batteries and Recent Progress in Battery Thermal Management Systems: A Review,” *Energy Conversion and Management*, Vol. 150, Oct. 2017, pp. 304–330.
https://doi.org/10.1016/j.enconman.2017.08.016

[15] Sun, H., and Dixon, R., “Development of Cooling Strategy for an Air Cooled Lithium-Ion Battery Pack,” *Journal of Power Sources*, Vol. 272, Dec. 2014, pp. 404–414.
https://doi.org/10.1016/j.jpowsour.2014.08.107

[16] Mohammadian, S. K., and Zhang, Y., “Thermal Management Optimization of an Air-Cooled Li-Ion Battery Module Using Pin-Fin Heat Sinks for Hybrid Electric Vehicles,” *Journal of Power Sources*, Vol. 273, Jan. 2015, pp. 431–439.
https://doi.org/10.1016/j.jpowsour.2014.09.110

[17] Mohammadian, S. K., Rassoulinejad-Mousavi, S. M., and Zhang, Y., “Thermal Management Improvement of an Air-Cooled High-Power Lithium-Ion Battery by Embedding Metal Foam,” *Journal of Power Sources*, Vol. 296, Nov. 2015, pp. 305–313.
https://doi.org/10.1016/j.jpowsour.2015.07.056

[18] Mohammadian, S. K., and Zhang, Y., “Cumulative Effects of Using Pin Fin Heat Sink and Porous Metal Foam on Thermal Management of Lithium-Ion Batteries,” *Applied Thermal Engineering*, Vol. 118, May 2017, pp. 375–384.
https://doi.org/10.1016/j.applthermaleng.2017.02.121

[19] Yu, K., Yang, X., Cheng, Y., and Li, C., “Thermal Analysis and Two-Directional Air Flow Thermal Management for Lithium-Ion Battery Pack,” *Journal of Power Sources*, Vol. 270, Dec. 2014, pp. 193–200.
https://doi.org/10.1016/j.jpowsour.2014.07.086

[20] Wang, T., Tseng, K. J., Zhao, J., and Wei, Z., “Thermal Investigation of Lithium-Ion Battery Module with Different Cell Arrangement Structures and Forced Air-Cooling Strategies,” *Applied Energy*, Vol. 134, Dec. 2014, pp. 229–238.
https://doi.org/10.1016/j.apenergy.2014.08.013

[21] Fathabadi, H., "A Novel Design Including Cooling Media for Lithium-Ion Batteries Pack Used in Hybrid and Electric Vehicles," *Journal of Power Sources*, Vol. 245, Jan. 2014, pp. 495–500. https://doi.org/10.1016/j.jpowsour.2013.06.160

[22] Fan, L., Khodadadi, J. M., and Pesaran, A. A., "A Parametric Study on Thermal Management of an Air-Cooled Lithium-Ion Battery Module for Plug-In Hybrid Electric Vehicles," *Journal of Power Sources*, Vol. 238, Sept. 2013, pp. 301–312. https://doi.org/10.1016/j.jpowsour.2013.03.050

[23] Yang, N., Zhang, X., Li, G., and Hua, D., "Assessment of the Forced Air-Cooling Performance for Cylindrical Lithium-Ion Battery Packs: A Comparative Analysis Between Aligned and Staggered Cell Arrangements," *Applied Thermal Engineering*, Vol. 80, April 2015, pp. 55–65. https://doi.org/10.1016/j.applthermaleng.2015.01.049

[24] Tong, W., Somasundaram, K., Birgersson, E., Mujumdar, A. S., and Yap, C., "Thermo-Electrochemical Model for Forced Convection Air Cooling of a Lithium-Ion Battery Module," *Applied Thermal Engineering*, Vol. 99, April 2016, pp. 672–682. https://doi.org/10.1016/j.applthermaleng.2016.01.050

[25] Yang, T., Yang, N., Zhang, X., and Li, G., "Investigation of the Thermal Performance of Axial Flow Air Cooling for the Lithium-Ion Battery Pack," *International Journal of Thermal Sciences*, Vol. 108, Oct. 2016, pp. 132–144. https://doi.org/10.1016/j.ijthermalsci.2016.05.009

[26] Saw, L. H., Ye, Y., Tay, A. O., Chong, W. T., Kuan, S. H., and Yew, M. C., "Computational Fluid Dynamic and Thermal Analysis of Lithium-Ion Battery Pack with Air Cooling," *Applied Energy*, Vol. 177, Sept. 2016, pp. 783–792. https://doi.org/10.1016/j.apenergy.2016.05.122

[27] Zhu, C., Li, X., Song, L., and Xiang, L., "Development of a Theoretically Based Thermal Model for Lithium Ion Battery Pack," *Journal of Power Sources*, Vol. 223, Feb. 2013, pp. 155–164. https://doi.org/10.1016/j.jpowsour.2012.09.035

[28] Wang, T., Tseng, K. J., and Zhao, J., "Development of Efficient Air-Cooling Strategies for Lithium-Ion Battery Module Based on Empirical Heat Source Model," *Applied Thermal Engineering*, Vol. 90, Nov. 2015, pp. 521–529. https://doi.org/10.1016/j.applthermaleng.2015.07.033

[29] Lan, C., Xu, J., Qiao, Y., and Ma, Y., "Thermal Management for High Power Lithium-Ion Battery by Mini Channel Aluminum Tubes," *Applied Thermal Engineering*, Vol. 101, May 2016, pp. 284–292. https://doi.org/10.1016/j.applthermaleng.2016.02.070

[30] Zhang, T., Gao, Q., Wang, G., Gu, Y., Wang, Y., and Bao, W., "Investigation on the Promotion of Temperature Uniformity for the Designed Battery Pack with Liquid Flow in Cooling Process," *Applied Thermal Engineering*, Vol. 116, April 2017, pp. 655–662. https://doi.org/10.1016/j.applthermaleng.2017.01.069

[31] Tong, W., Somasundaram, K., Birgersson, E., Mujumdar, A. S., and Yap, C., "Numerical Investigation of Water Cooling for a Lithium-Ion Bipolar Battery Pack," *International Journal of Thermal Sciences*, Vol. 94, Aug. 2015, pp. 259–269. https://doi.org/10.1016/j.ijthermalsci.2015.03.005

[32] Huo, Y., Rao, Z., Liu, X., and Zhao, J., "Investigation of Power Battery Thermal Management by Using Mini-Channel Cold Plate," *Energy Conversion and Management*, Vol. 89, Jan. 2015, pp. 387–395. https://doi.org/10.1016/j.enconman.2014.10.015

[33] Qian, Z., Li, Y., and Rao, Z., "Thermal Performance of Lithium-Ion Battery Thermal Management System by Using Mini-Channel Cooling," *Energy Conversion and Management*, Vol. 126, Oct. 2016, pp. 622–631. https://doi.org/10.1016/j.enconman.2016.08.063

[34] Jin, L. W., Lee, P. S., Kong, X. X., Fan, Y., and Chou, S. K., "Ultra-Thin Mini Channel LCP for EV Battery Thermal Management," *Applied Energy*, Vol. 113, Jan. 2014, pp. 1786–1794. https://doi.org/10.1016/j.apenergy.2013.07.013

[35] Jarrett, A., and Kim, I. Y., "Design Optimization of Electric Vehicle Battery Cooling Plates for Thermal Performance," *Journal of Power Sources*, Vol. 196, No. 23, Dec. 2011, pp. 10359–10368. https://doi.org/10.1016/j.jpowsour.2011.06.090

[36] Jarrett, A., and Kim, I. Y., "Influence of Operating Conditions on the Optimum Design of Electric Vehicle Battery Cooling Plates," *Journal of Power Sources*, Vol. 245, Jan. 2014, pp. 644–655. https://doi.org/10.1016/j.jpowsour.2013.06.114

[37] Zhao, J., Rao, Z., and Li, Y., "Thermal Performance of Mini-Channel Liquid Cooled Cylinder Based Battery Thermal Management for Cylindrical Lithium-Ion Power Battery," *Energy Conversion and Management*, Vol. 103, Oct. 2015, pp. 157–165. https://doi.org/10.1016/j.enconman.2015.06.056

[38] Huo, Y., and Rao, Z., "The Numerical Investigation of Nanofluid Based Cylinder Battery Thermal Management Using Lattice Boltzmann Method," *International Journal of Heat and Mass Transfer*, Vol. 91, Dec. 2015, pp. 374–384. https://doi.org/10.1016/j.ijheatmasstransfer.2015.07.128

[39] Yang, X.-H., Tan, S.-C., and Liu, J., "Thermal Management of Li-Ion Battery with Liquid Metal," *Energy Conversion and Management*, Vol. 117, June 2016, pp. 577–585. https://doi.org/10.1016/j.enconman.2016.03.054

[40] van Gils, R. W., Danilov, D., Notten, P. H. L., Speetjens, M. F. M., and Nijmeijer, H., "Battery Thermal Management by Boiling Heat-Transfer," *Energy Conversion and Management*, Vol. 79, March 2014, pp. 9–17. https://doi.org/10.1016/j.enconman.2013.12.006

[41] Al-Zareer, M., Dincer, I., and Rosen, M. A., "Heat and Mass Transfer Modeling and Assessment of a New Battery Cooling System," *International Journal of Heat and Mass Transfer*, Vol. 126, Nov. 2018, pp. 765–778. https://doi.org/10.1016/j.ijheatmasstransfer.2018.04.157

[42] An, Z., Jia, L., Li, X., and Ding, Y., "Experimental Investigation on Lithium-Ion Battery Thermal Management Based on Flow Boiling in Mini-Channel," *Applied Thermal Engineering*, Vol. 117, May 2017, pp. 534–543. https://doi.org/10.1016/j.applthermaleng.2017.02.053

[43] Nazari, M. A., Ahmadi, M. H., Ghasempour, R., and Shafii, M. B., "How to Improve the Thermal Performance of Pulsating Heat Pipes: A Review on Working Fluid," *Renewable and Sustainable Energy Reviews*, Vol. 91, Aug. 2018, pp. 630–638. https://doi.org/10.1016/j.rser.2018.04.042

[44] Krishna, J., Kishore, P. S., and Solomon, A. B., "Heat Pipe with Nano Enhanced-PCM for Electronic Cooling Application," *Experimental Thermal and Fluid Science*, Vol. 81, Feb. 2017, pp. 84–92. https://doi.org/10.1016/j.expthermflusci.2016.10.014

[45] Hodot, R., Sartre, V., Lefevre, F., and Sarno, C., "Modeling and Experimental Tests of a Loop Heat Pipe for Aerospace Applications," *Journal of Thermophysics and Heat Transfer*, Vol. 30, No. 1, 2016, pp. 182–191. https://doi.org/10.2514/1.T4551

[46] Pise, G. A., Salve, S. S., Pise, A. T., and Pise, A. A., "Investigation of Solar Heat Pipe Collector Using Nano Fluid and Surfactant," *Energy Procedia*, Vol. 90, Dec. 2016, pp. 481–491. https://doi.org/10.1016/j.egypro.2016.11.215

[47] Wang, C., Chen, J., Qiu, S., Tian, W., Zhang, D., and Su, G. H., "Performance Analysis of Heat Pipe Radiator Unit for Space Nuclear Power Reactor," *Annals of Nuclear Energy*, Vol. 103, May 2017, pp. 74–84. https://doi.org/10.1016/j.anucene.2017.01.015

[48] Rao, Z., Wang, S., Wu, M., Lin, Z., and Li, F., "Experimental Investigation on Thermal Management of Electric Vehicle Battery with Heat Pipe," *Energy Conversion and Management*, Vol. 65, Jan. 2013, pp. 92–97. https://doi.org/10.1016/j.enconman.2012.08.014

[49] Ji, Y., Ma, H., Su, F., and Wang, G., "Particle Size Effect on Heat Transfer Performance in an Oscillating Heat Pipe," *Experimental Thermal and Fluid Science*, Vol. 35, No. 4, 2011, pp. 724–727. https://doi.org/10.1016/j.expthermflusci.2011.01.007

[50] Burban, G., Ayel, V., Alexandre, A., Lagonotte, P., Bertin, Y., and Romestant, C., "Experimental Investigation of a Pulsating Heat Pipe for Hybrid Vehicle Applications," *Applied Thermal Engineering*, Vol. 50, No. 1, 2013, pp. 94–103. https://doi.org/10.1016/j.applthermaleng.2012.05.037

[51] Rao, Z., Huo, Y., and Liu, X., "Experimental Study of an OHP-Cooled Thermal Management System for Electric Vehicle Power Battery," *Experimental Thermal and Fluid Science*, Vol. 57, Sept. 2014, pp. 20–26. https://doi.org/10.1016/j.expthermflusci.2014.03.017

[52] Putra, N., Ariantara, B., and Pamungkas, R. A., "Experimental Investigation on Performance of Lithium-Ion Battery Thermal Management System Using Flat Plate Loop Heat Pipe for Electric Vehicle Application," *Applied Thermal Engineering*, Vol. 99, April 2016, pp. 784–789. https://doi.org/10.1016/j.applthermaleng.2016.01.123

[53] Chen, S. C., Wan, C. C., and Wang, Y. Y., "Thermal Analysis of Lithium-Ion Batteries," *Journal of Power Sources*, Vol. 140, No. 1, 2005, pp. 111–124. https://doi.org/10.1016/j.jpowsour.2004.05.064

[54] Ma, H. B., Borgmeter, B., Cheng, P., and Zhang, Y., "Heat Transport Capability in an Oscillating Heat Pipe," *Journal of Heat Transfer*, Vol. 130, No. 8, 2008, Paper 081501. https://doi.org/10.1115/1.2909081

[55] Xiao, M., and Choe, S.-Y., "Theoretical and Experimental Analysis of Heat Generations of a Pouch Type $LiMn_2O_4$/Carbon High Power Li-Polymer Battery," *Journal of Power Sources*, Vol. 241, Nov. 2013, pp. 46–55. https://doi.org/10.1016/j.jpowsour.2013.04.062

[56] Ye, Y., Shi, Y., Cai, N., Lee, J., and He, X., "Electro-Thermal Modeling and Experimental Validation for Lithium Ion Battery," *Journal of Power*

*Sources*, Vol. 199, Feb. 2012, pp. 227–238.
https://doi.org/10.1016/j.jpowsour.2011.10.027

[57] Lai, Y., Du, S., Ai, L., Ai, L., Cheng, Y., and Tang, Y., "Insight into Heat Generation of Lithium Ion Batteries Based on the Electrochemical-Thermal Model at High Discharge Rates," *International Journal of Hydrogen Energy*, Vol. 40, No. 38, 2015, pp. 13039–13049.
https://doi.org/10.1016/j.ijhydene.2015.07.079

[58] Zhang, X., "Thermal Analysis of a Cylindrical Lithium-Ion Battery," *Electrochimica Acta*, Vol. 56, No. 3, 2011, pp. 1246–1255.
https://doi.org/10.1016/j.electacta.2010.10.054

[59] Nyman, A., Zavalis, T. G., Elger, R., Behm, M., and Lindbergh, G., "Analysis of the Polarization in a Li-Ion Battery Cell by Numerical Simulations," *Journal of Electrochemical Society*, Vol. 157, No. 11, 2010, pp. A1236–A1246.
https://doi.org/10.1149/1.3486161

[60] Gu, W. B., and Wang, C. Y., "Thermal-Electrochemical Modeling of Battery System," *Journal of Electrochemical Society*, Vol. 147, No. 8, 2000, pp. 2910–2922.
https://doi.org/10.1149/1.1393625

[61] Bernardi, D., "A General Energy Balance for Battery Systems," *Journal of Electrochemical Society*, Vol. 132, No. 1, 1985, pp. 5–12.
https://doi.org/10.1149/1.2113792

[62] Karimi, G., and Li, X., "Thermal Management of Lithium-Ion Batteries for Electric Vehicles," *International Journal of Energy Research*, Vol. 37, No. 1, 2013, pp. 13–24.
https://doi.org/10.1002/er.v37.1

[63] Inui, Y., Kobayashi, Y., Watanabe, Y., Watase, Y., and Kitamura, Y., "Simulation of Temperature Distribution in Cylindrical and Prismatic Lithium Ion Secondary Batteries," *Energy Conversion and Management*, Vol. 48, No. 7, 2007, pp. 2103–2109.
https://doi.org/10.1016/j.enconman.2006.12.012

[64] Bergman, T. L., Lavine, A. S., Incropera, F. P., and DeWitt, D. P., *Introduction to Heat Transfer*, 6th ed., Wiley, Hoboken, NJ, 2011, Chaps. 6, 8.

[65] Fuller, T. F., Doyle, M., and Newman, J., "Simulation and Optimization of the Dual Lithium Ion Insertion Cell," *Journal of Electrochemical Society*, Vol. 141, No. 1, 1994, pp. 1–10.
https://doi.org/10.1149/1.2054684

[66] Doyle, M., "Modeling of Galvanostatic Charge and Discharge of the Lithium/Polymer/Insertion Cell," *Journal of Electrochemical Society*, Vol. 140, No. 6, 1993, pp. 1526–1533.
https://doi.org/10.1149/1.2221597

[67] Subramanian, V. R., Ritter, J. A., and White, R. E., "Approximate Solutions for Galvanostatic Discharge of Spherical Particles I. Constant Diffusion Coefficient," *Journal of Electrochemical Society*, Vol. 148, No. 11, 2001, pp. E444–E449.
https://doi.org/10.1149/1.1409397

[68] Subramanian, V. R., Tapriyal, D., and White, R. E., "A Boundary Condition for Porous Electrodes," *Electrochemical Solid-State Letters*, Vol. 7, No. 9, 2004, pp. A259–A263.
https://doi.org/10.1149/1.1773751

[69] Guo, M., Sikha, G., and White, R. E., "Single-Particle Model for a Lithium-Ion Cell: Thermal Behavior," *Journal of Electrochemical Society*, Vol. 158, No. 2, 2011, pp. A122–A132.
https://doi.org/10.1149/1.3521314

[70] Dubey, A. M., Ram, R., and Yadav, A. K., "Ion Cell Performance Using Single Particle Representation of Battery Electrode," *Journal of Electroanalytical Chemistry*, Vol. 768, May 2016, pp. 11–17.
https://doi.org/10.1016/j.jelechem.2016.02.018

[71] Santhanagopalan, S., Guo, Q., Ramadass, P., and White, R. E., "Review of Models for Predicting the Cycling Performance of Lithium Ion Batteries," *Journal of Power Sources*, Vol. 156, No. 2, 2006, pp. 620–628.
https://doi.org/10.1016/j.jpowsour.2005.05.070

[72] Wang, C. Y., Gu, W. B., and Liaw, B. Y., "Micro-Macroscopic Coupled Modeling of Batteries and Fuel Cells," *Journal of Electrochemical Society*, Vol. 145, No. 10, 1998, pp. 3407–3147.
https://doi.org/10.1149/1.1838820

[73] Shah, A. J., "Exergy-Based Analysis and Optimization of Computer Thermal Management Systems," Ph.D. Dissertation, Engineering-Mechanical Engineering, Univ. of California, Berkeley, CA, 2005.

[74] Rang, T., Liu, X.-H., Hwang, Y., and Ma, F., "Performance Analysis of Ventilation Systems with Desiccant Wheel Cooling Based on Exergy Destruction," *Energy Conversion and Management*, Vol. 123, Sept. 2016, pp. 265–279.
https://doi.org/10.1016/j.enconman.2016.06.013

[75] Mohammadi, A., Ahmadi, M. H., Ahmadi, M., Joda, F., Valero, A., and Uson, S., "Exergy Analysis of a Combined Cooling, Heating and Power System Integrated with Wind Turbine and Compressed Air Energy Storage System," *Energy Conversion and Management*, Vol. 131, Jan. 2017, pp. 69–78.
https://doi.org/10.1016/j.enconman.2016.11.003

[76] Singh, K., and Das, R., "Exergy Optimization of Cooling Tower for HGSHP and HVAC Applications," *Energy Conversion and Management*, Vol. 136, March 2017, pp. 418–430.
https://doi.org/10.1016/j.enconman.2017.01.024

[77] Shah, A. J., Carey, V. P., Bash, C. E., and Patel, C. D., "Exergy Analysis of Data Center Thermal Management Systems," *Energy Efficient Thermal Management of Data Centers*, Vol. 130, 2008, Paper 021401.
https://doi.org/10.1115/1.2787024